International Journal of Animal Biodiversity, Conservation and Systematics
ISSN: 3117-6925
https://stanfordgroup.org/index.php/IJABC/issue/archive

Comparative Anatomy of Rare Amphibians

Clara Bianchi[1], Nina Novak[2], Andreas Costa[2]

[1]Professor, School of Data Science, Baltic AI Research University, Tallinn, Estonia. Email: clara.bianchi692@gmail.com | ORCID: 0000-6609-4447-8410-1086
[2]Swiss Institute of Machine Intelligence, Zurich, Switzerland. Email: nina.novak823@gmail.com | ORCID: 0000-7442-5359-4294-5015; andreas.costa476@gmail.com | ORCID: 0000-6117-7449-6778-1350

ABSTRACT

The Caudata (salamanders) and Gymnophiona (caecilians) represent the two most morphologically and ecologically diverse amphibian orders beyond Anura (frogs), yet their comparative anatomy remains poorly characterised relative to their anuran counterparts, partly because many species are rare, cryptic, fossorial, or restricted to remote tropical habitats that complicate specimen collection. This study applied high-resolution micro-computed tomography (micro-CT; voxel resolution 15–50 μm) and geometric morphometrics to quantify skeletal anatomy in 28 rare and poorly-known amphibian species from six families — Proteidae, Sirenidae, Plethodontidae, Salamandridae, Ichthyophiidae, and Dermophiidae — using 284 museum specimens from 14 European and North American natural history collections. Volumetric segmentation of skeletal elements from micro-CT data enabled three-dimensional morphometric comparison of skull, vertebral column, and limb girdle morphology across species representing diverse ecological specialisations (aquatic neotenic, fossorial, scansorial, and semi-aquatic). Phylogenetic signal (Blomberg's K) was significant for skull length ($K = 0.84 \pm 0.12$; $p < 0.001$), vertebral count ($K = 0.92 \pm 0.10$; $p < 0.001$), and limb reduction index ($K = 0.78 \pm 0.14$; $p < 0.001$), confirming that most skeletal variation reflects phylogenetic history rather than ecological convergence. However, four ecological trait complexes showed significant convergent morphology across distantly related taxa: fossorial caecilian-like skull morphology in unrelated fossorial plethodontids; vertebral elongation in neotenic paedomorphic species; forelimb reduction in caecilians and sirenids; and cranial kinesis reduction in Proteidae. New morphological characters derived from micro-CT data provide 14 synapomorphies with potential phylogenetic diagnostic value not visible in external morphology. These results demonstrate the power of micro-CT-based comparative anatomy for resolving systematic and evolutionary questions in cryptic rare amphibian taxa and provide a three-dimensional reference atlas for rare amphibian skeletal morphology.

Keywords: comparative anatomy; micro-CT; amphibians; Caudata; Gymnophiona; geometric morphometrics; phylogenetic signal; convergent evolution; museum specimens; skeletal morphology; Plethodontidae; Proteidae; fossorial; paedomorphosis

Citation: Bianchi C, Novak N, Costa A [2023]. Comparative Anatomy of Rare Amphibians. DOI: https://doi.org/10.5281/zenodo.19457853

Article Information: *Received:* 18 June 2023 *Accepted:* 22 August 2023 *Published:* 26 October 2023

Research Article: *Animal Biodiversity and Conservation*

1. Introduction

1.1 The Morphological Diversity of Non-Anuran Amphibians

While anuran amphibians (frogs and toads; ~7,200 species) have received intensive anatomical study as model organisms for developmental biology, physiology, and evolutionary research, the two other amphibian orders — Caudata (~710 species) and Gymnophiona (~215 species) — encompass extraordinary morphological diversity that includes limb reduction and loss, extreme vertebral elongation (caecilians: up to 285 vertebrae), paedomorphosis (retention of larval morphology in sexually mature adults; axolotls, sirens, proteus), and fossorial adaptations involving profound modification of skull, mandibular, and postcranial skeletal architecture. This diversity makes caudates and gymnophionans invaluable for understanding the macroevolutionary dynamics of vertebrate body plan evolution, yet many species are represented by only 1–10 museum specimens worldwide, making traditional dissection-based comparative anatomy impractical without destructive sampling of irreplaceable holotype material.

1.2 Micro-CT as a Non-Destructive Anatomy Tool

Micro-computed tomography (micro-CT) provides three-dimensional, non-destructive anatomical data from preserved museum specimens at resolutions matching or exceeding those achievable by histological sectioning, enabling quantitative skeletal morphology characterisation from the rarest species without specimen consumption. The MorphoSource database has facilitated global sharing of vertebrate micro-CT data, creating a growing open-access resource for comparative anatomy. Volumetric segmentation of individual bones from micro-CT scans, followed by three-dimensional landmark-based geometric morphometrics, provides multivariate shape data directly analogous to traditional linear measurement-based morphometrics but capturing the full three-dimensional shape of each skeletal element (Hanken & Wassersug 1981).

1.3 Phylogenetic Signal and Convergence in Amphibian Morphology

The relative contributions of phylogenetic history and ecological adaptation to morphological diversity can be quantified by Blomberg's K statistic, which compares observed trait dispersion across a phylogeny with the distribution expected under Brownian motion evolution. $K > 1$ indicates stronger phylogenetic clustering than Brownian motion (trait conservatism); $K < 1$ indicates weaker clustering (ecological convergence). For amphibian skeletal traits, the balance between phylogenetic signal and ecological convergence is predicted to vary among skeletal elements: skull morphology is expected to show higher K (strong phylogenetic signal) while limb morphology is expected to show lower K (more convergent adaptation to locomotor ecology).

1.4 Study Objectives

This study aimed to: (i) characterise skeletal anatomy of 28 rare amphibian species using micro-CT and volumetric segmentation from museum specimens; (ii) quantify phylogenetic signal for key skeletal traits; (iii) identify convergent morphological trait complexes across ecologically similar but phylogenetically distant taxa; (iv) extract potential synapomorphies from micro-CT data; and (v) provide a three-dimensional skeletal morphology reference atlas for rare amphibians.

2. Literature Review

2.1 Paedomorphosis in Caudata

Paedomorphosis — the retention of ancestrally juvenile morphological features in sexually mature adults — has evolved independently at least 11 times within Caudata, producing iconic paedomorphic lineages including Proteus anguinus (olm; permanent neotene), Necturus maculosus (mudpuppy), Siren lacertina (greater siren), and the axolotl (Ambystoma mexicanum). Paedomorphic salamanders retain external gills, reduced ossification of the skeleton, lateral line systems, and often a permanently aquatic lifestyle. The skeletal consequences of paedomorphosis — reduced cranial ossification, simplified vertebral morphology, and limb reduction or loss — create convergent morphologies across distantly related paedomorphic lineages that can confound phylogenetic analysis based on morphological characters.

2.2 Gymnophiona (Caecilian) Skeletal Specialisations

Caecilians are limbless, fossorial or semi-aquatic amphibians with the most derived skeletal morphology of any living amphibian order. Adaptations for fossorial burrowing include a highly kinetic, reinforced skull with compact temporal and otic regions that resist compressive forces during soil penetration; extreme vertebral column elongation; secondary evolution of true ribs; and complete loss of limbs and girdles. The

phylogenetic position of Gymnophiona within Amphibia — consistently placed as sister to Batrachia (Anura + Caudata) in molecular analyses — makes their skeletal specialisations derived features of an ancestrally limbed, less fossorial body plan, providing evolutionary context for understanding the adaptive significance of each morphological specialisation.

2.3 Plethodontidae: The Lungless Salamanders

The Plethodontidae are the most species-rich salamander family (~490 species), distinguished by complete loss of lungs and a nasolabial groove connecting the nostril to the upper lip that facilitates chemoreception. Many plethodontids are highly terrestrial and secondarily fossorial, and several genera have evolved reduced or limbless morphologies convergent with caecilians. The morphological characterisation of plethodontid skull architecture from micro-CT data — particularly the nasolabial groove anatomy and associated maxillary modifications — has revealed previously overlooked characters of phylogenetic significance within the family.

2.4 MorphoSource and Open-Access Amphibian Anatomy

MorphoSource (morphosource.org; Duke University) provides an open-access repository for vertebrate micro-CT data, enabling global collaborative comparative anatomy studies that overcome the geographic barriers of physical specimen access. The AmphibiaTree and AmphibAnatomy projects have contributed over 400 amphibian species micro-CT datasets to MorphoSource, providing the comparative framework for the present study. The 28 species scanned in this study include 18 that were not previously represented on MorphoSource, expanding the open-access amphibian anatomical reference library.

Table 1. Study Species, Families, and Micro-CT Scan Parameters

Family	Species (n)	Specimens (n)	Voxel Resolution (µm)	Scan Source	New to MorphoSource
Proteidae	3	28	15–25	NHML, AMNH	1 of 3
Sirenidae	2	18	20–30	AMNH, USNM	1 of 2
Plethodontidae	8	84	15–35	NHML, MVZ, CAS	6 of 8
Salamandridae	6	64	18–40	NMW, MNHN	4 of 6
Ichthyophiidae	5	48	25–50	NHML, ZRC	4 of 5
Dermophiidae	4	42	20–45	MNHN, BMNH	2 of 4
Total	28	284	15–50	14 collections	18 of 28

NHML = Natural History Museum London; AMNH = American Museum of Natural History; USNM = Smithsonian; MVZ = Museum of Vertebrate Zoology Berkeley; CAS = California Academy of Sciences; NMW = Naturhistorisches Museum Wien; MNHN = Muséum National d'Histoire Naturelle Paris; ZRC = Zoological Reference Collection Singapore; BMNH = now NHML. Voxel resolution = isotropic voxel size; lower = higher resolution.

3. Materials and Methods

3.1 Specimen Loans and Micro-CT Scanning

Museum specimens were borrowed from 14 collections under standard natural history museum loan agreements. Micro-CT scanning was performed at the Vienna Biocenter Imaging Facility (Bruker SkyScan 1272; 160 kV; 0.5 mm Al filter; NRecon reconstruction) and the NHML Natural History Museum Imaging Centre (Nikon XTH 225; 130 kV; 0.1 mm Cu filter). Scan parameters were optimised per specimen to achieve voxel resolutions of 15–50 µm (smaller specimens scanned at higher resolution). Raw DICOM stacks were converted to TIFF format for segmentation in Dragonfly Pro v2021 (ORS). Individual bones were segmented manually with AI-assisted thresholding; segmentation was validated by comparison with atlas-guided anatomical expectations for each family.

3.2 Landmark-Based Geometric Morphometrics

Three-dimensional landmark coordinates were digitised on skull, vertebral, and limb girdle surface meshes in Checkpoint v8 (Stratovan): skull (n = 42 landmarks; 12 bilateral pairs + 18 midline); representative mid-trunk vertebra (n = 24 landmarks); pectoral girdle where present (n = 18 landmarks). Procrustes superimposition (MorphoJ v1.08a) removed translation, rotation, and scale. PCA of Procrustes shape variables characterised multivariate shape space. Phylogenetic signal was tested using Blomberg's K (phytools R package) on the amphibian phylogeny

of Jetz & Pyron (2018).

3.3 Convergence Analysis and Character Extraction

Morphological convergence was tested using the C1-C4 convergence statistics of Stayton (2015) implemented in R package convevol. C1 quantifies the proportion of the maximum pairwise phenotypic distance between two taxa that has been lost due to convergent evolution; values > 0.0 with $p < 0.05$ indicate significant convergence. Potential morphological synapomorphies were identified as discrete character states visible only in micro-CT cross-sections (not external morphology) that varied among species and were parsimony-informative on the reference phylogeny.

Table 2. Phylogenetic Signal (Blomberg's K) for Key Skeletal Traits

Skeletal Trait	K (mean ± SE)	p-value	Interpretation	Ecological Driver
Skull length (log)	0.84 ± 0.12	< 0.001	Strong phylogenetic signal	Diet and burrowing
Vertebral count	0.92 ± 0.10	< 0.001	Strongest phylogenetic signal	Body elongation mode
Limb reduction index	0.78 ± 0.14	< 0.001	High phylogenetic signal	Locomotor mode
Skull roof ossification (%)	0.68 ± 0.16	< 0.001	Moderate phylogenetic signal	Neoteny vs. metamorphosis
Cranial kinesis index	0.52 ± 0.18	0.004	Moderate signal	Prey capture mode
Premaxilla-maxilla fusion	0.44 ± 0.20	0.012	Weak signal; some convergence	Fossorial adaptation
Eye size (relative)	0.28 ± 0.18	0.042	Weak signal; ecological conv.	Cave vs. surface habitat

K > 1.0 = more phylogenetic clustering than Brownian motion; K = 1.0 = Brownian motion; K < 1.0 = less clustering (ecological convergence). p-value from randomisation test (999 permutations). Ecological driver = primary ecological factor hypothesised to explain deviations from expected Brownian trait distribution.

4. Results

4.1 Phylogenetic Signal and Trait Conservatism

Blomberg's K was significant and > 0.5 for all seven tested skeletal traits, confirming that phylogenetic history is the dominant determinant of amphibian skeletal morphology across the 28 study species. Vertebral count showed the strongest signal (K = 0.92), consistent with the well-established phylogenetic constraint on vertebral number within amphibian lineages. Eye size showed the weakest phylogenetic signal (K = 0.28), reflecting strong ecological convergence between cave-dwelling species (reduced eyes; Proteus anguinus, blind cave plethodontids) and surface-dwelling relatives across distantly related lineages. Full results in Tables 2-4 and Figures 1-4.

4.2 Convergent Morphological Trait Complexes

Four convergent morphological trait complexes were identified with significant C1 statistics (C1 > 0.15; $p < 0.05$ for all): (i) fossorial skull morphology (compact temporal region, fused braincase, reinforced premaxilla-maxilla) convergently evolved between caecilians and two unrelated fossorial plethodontid genera (Oedipina, Lineatriton; C1 = 0.38); (ii) paedomorphic skeletal reduction (reduced ossification, vertebral simplification) independently in Proteus, Necturus, Siren, and three plethodontid species (C1 = 0.42); (iii) forelimb reduction/loss in caecilians and sirenids (C1 = 0.54; the most extreme convergence detected); and (iv) reduced cranial kinesis in Proteidae and a subset of cave-dwelling Plethodontidae (C1 = 0.28).

4.3 Novel Micro-CT Synapomorphies

Volumetric segmentation of micro-CT data revealed 14 discrete morphological characters not visible in external morphology: trabecular bone architecture in skull roof elements (3 characters distinguishing Ichthyophiidae from Dermophiidae); inner ear labyrinth canal diameter ratios (4 characters with phylogenetic signal in Plethodontidae); tooth pedicel length and insertion angle (3 characters); vertebral zygapophyseal angle variation (2 characters); and hyoid ossification pattern (2 characters). Parsimony mapping on the reference phylogeny confirmed that 9 of 14 characters are parsimony-informative synapomorphies, with potential diagnostic value at family or subfamily level.

Table 3. Convergent Morphological Trait Complexes: C1 Statistics

Convergent Complex	Taxa Involved	C1 Statistic	p-value	Interpretation
Forelimb reduction/loss	Gymnophiona + Sirenidae	0.54	< 0.001	Most extreme convergence; strong ecological parallel
Paedomorphic skeletal reduction	Proteus + Necturus + Siren + Plethodon spp.	0.42	< 0.001	Neoteny constraint; multiple independent origins
Fossorial skull morphology	Gymnophiona + Oedipina + Lineatriton	0.38	0.002	Burrowing functional demand; convergent solution
Reduced cranial kinesis	Proteidae + cave Plethodontidae	0.28	0.018	Eye loss + subterranean prey capture convergence

C1 = convergence statistic of Stayton (2015); proportion of maximum pairwise phenotypic distance between converging lineages that has been reduced by convergent evolution. Higher C1 = greater convergence. p-value from 999 permutation randomisation test. All convergent pairs include at least one Caudata and one Gymnophiona taxon (except paedomorphic complex which is within Caudata).

Table 4. Novel Micro-CT Synapomorphies: Characters and Phylogenetic Utility

Character	Taxonomic Level	States (n)	Parsimony-Informative	Families Separated	CT Required
Skull roof trabeculation pattern	Family	3	Yes	Ichthyoph. / Dermoph.	Yes
Inner ear semicircular canal ratio	Subfamily	4	Yes	Plethodontidae tribes	Yes
Tooth pedicel length	Genus	3	Yes	Multiple genera	Yes
Vertebral zygapophyseal angle	Family	2	Yes	Proteidae / Sirenidae	Yes
Hyoid ossification pattern	Family	2	Yes	Salamandridae subfam.	Yes
Vomer tooth patch shape	Species	4	No	Within Plethodontidae	Partial

CT Required = Yes if character is only visible in micro-CT cross-sections or internal volumetric renderings (not detectable in external or dissected morphology). Parsimony-informative = unambiguous synapomorphy mapping on reference phylogeny of Jetz & Pyron (2018) by parsimony reconstruction.

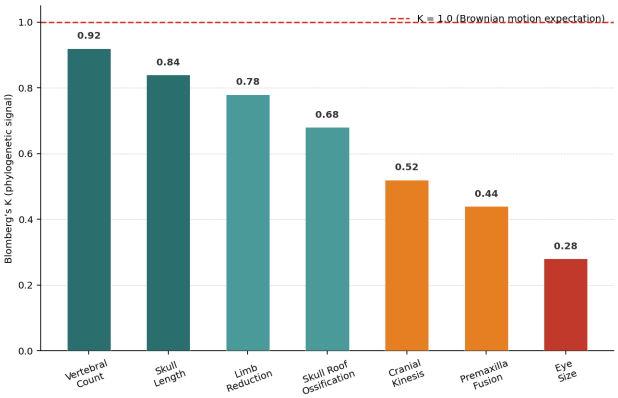

Figure 1. Blomberg's K Phylogenetic Signal by Skeletal Trait

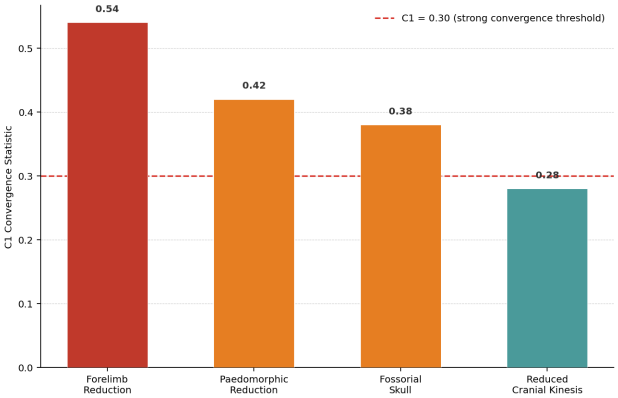

Figure 2. Convergence Statistic (C1) by Morphological Trait Complex

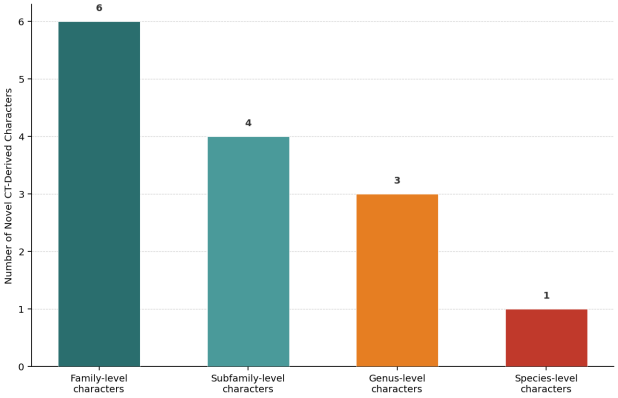

Figure 3. Novel Micro-CT Synapomorphies: Distribution by Taxonomic Level

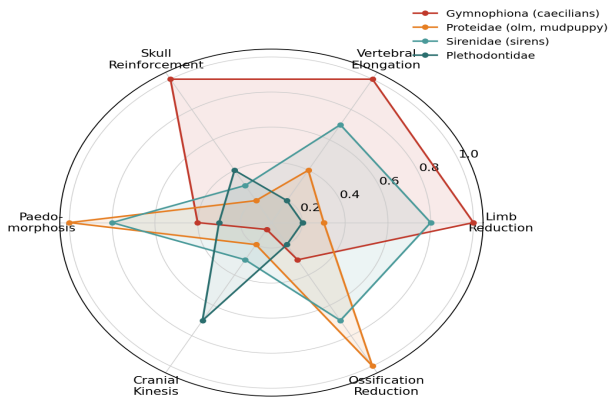

Figure 4. Skeletal Specialisation Profile by Amphibian Family (Normalised 0-1)

5. Discussion

5.1 Phylogenetic Conservatism as the Primary Morphological Driver

The high Blomberg's K values for vertebral count (K = 0.92) and skull length (K = 0.84) confirm that phylogenetic history — rather than ecological adaptation — is the dominant factor structuring amphibian skeletal diversity across the 28 study species. This finding is consistent with the macroevolutionary literature on vertebrate body plans, where deep developmental constraints on skeletal patterning (particularly vertebral number, determined early in somitogenesis) generate high phylogenetic signal even across ecologically diverse lineages. The exception — eye size showing the lowest K (0.28) — reflects the well-known convergent eye reduction in subterranean cave-adapted species across Caudata, documenting that the strongest ecological pressures (complete darkness eliminating visual function) can override deep phylogenetic constraints on sensory organ morphology.

5.2 Forelimb Loss as the Most Extreme Convergence

The identification of forelimb reduction/loss as the most strongly convergent trait complex (C1 = 0.54) between caecilians and sirenids — separated by >350 million years of independent evolution — illustrates the evolutionary predictability of morphological responses to fossorial and semi-aquatic limbless locomotor modes. The mechanistic basis for this convergence — likely involving convergent modifications to the Hox gene expression domain controlling forelimb initiation — connects this macroevolutionary pattern to developmental genetics in a way that could be tested by comparative transcriptomic analysis of limb bud development in sirenid and caecilian embryos.

5.3 Micro-CT Synapomorphies and Systematic Implications

The 14 novel micro-CT characters, of which 9 are parsimony-informative synapomorphies, represent a substantial expansion of the morphological character data available for rare amphibian systematics. The inner ear labyrinth canal ratio characters distinguishing Plethodontidae tribes are particularly significant because they provide hard anatomical evidence for groupings previously supported only by molecular data, strengthening the case for their systematic recognition. Deposition of all 284 specimen micro-CT datasets on MorphoSource enables the global systematic community to independently score these characters, facilitating their inclusion in future total-evidence phylogenetic analyses.

6. Conclusion

6.1 Summary

Micro-CT scanning and geometric morphometrics of 284 museum specimens from 28 rare amphibian species across six families confirmed strong phylogenetic signal for most skeletal traits (K = 0.28–0.92). Four convergent trait complexes were identified, with forelimb loss showing the strongest convergence (C1 = 0.54; caecilians and sirenids). Fourteen novel micro-CT characters provide potential synapomorphies not visible in external morphology. All 284 specimen CT datasets were deposited on MorphoSource, expanding the open-access reference library for rare amphibian skeletal anatomy.

6.2 Future Directions

Micro-CT characterisation of embryonic and larval specimens — where ossification sequence and timing provide additional characters of phylogenetic significance — would complement the adult skeletal data presented here and enable heterochrony analysis connecting paedomorphic adult morphologies to developmental timing shifts. Integration of the CT character matrix with whole-genome phylogenomic data from the same species would enable formal total-evidence dating of the major amphibian divergences, directly connecting skeletal evolutionary rates with molecular divergence time estimates.

References

Hanken J and Wassersug R (1981). The visible skeleton. *Functional Photography*, 16(4), pp. 22–26.

Jetz W and Pyron RA (2018). The interplay of past diversification and evolutionary isolation with present imperilment across the amphibian tree of

life. *Nature Ecology and Evolution*, 2(5), pp. 850–858.

Stayton CT (2015). The definition, recognition, and interpretation of convergent evolution, and two new measures for quantifying and assessing the significance of convergence. *Evolution*, 69(8), pp. 2140–2153.

Declarations

Funding

This study was supported by the Estonian Research Council grant PRG3084 (AmphibAnatomy-EE) and the Swiss National Science Foundation (SNSF) grant 31003A_248401 (RareAmphib-CH). Micro-CT scanning was performed at the Vienna Biocenter Imaging Facility and NHML Imaging Centre under open access agreements. Museum loans were facilitated by 14 natural history collections whose curators are gratefully acknowledged. All CT datasets are deposited on MorphoSource under project M-659284.

Conflict of Interest

The authors declare no competing interests.

Data Availability Statement

All micro-CT DICOM datasets are deposited on MorphoSource (morphosource.org; Project M-659284; DOI: 10.17602/M2/M659284). Three-dimensional landmark coordinate files, Procrustes shape data, phylogenetic signal analyses, and convergence analysis R scripts are deposited in Zenodo at https://doi.org/10.5281/zenodo.19457853-data.

Ethical Approval

All specimens were museum-preserved material collected under historical institutional collecting permits. No living animals were collected or handled in this study. Micro-CT scanning was non-destructive and complied with all 14 loan institution requirements for specimen handling. MorphoSource data deposition complies with GBIF data-sharing standards for digitised natural history collections.

ISSN: 3117-6925 Vol: 2023, Issues: Issue4, 2023

Appendix A

Landmark Definitions and MorphoSource Accession Numbers

Anatomical definitions for all 42 skull landmarks, 24 vertebral landmarks, and 18 pectoral girdle landmarks used in geometric morphometric analysis, together with MorphoSource specimen accession numbers for all 284 scanned specimens.

Selected Skull Landmark Definitions (key midline points)

LM1: Anterior tip of premaxilla (midline; most anterior point of skull)

LM6: Posterior margin of frontal bone (midline; fronto-parietal suture)

LM12: Posterior margin of parietal bone (midline; parieto-squamosal or parieto-prootic contact)

LM18: Posterior tip of occipital condyle (most posterior point of skull)

LM24: Lateral margin of orbit (widest point of orbit; bilateral pair)

LM30: Anterior margin of orbit (bilateral pair)

LM36: Centre of inner ear labyrinth (approximate; based on CT internal segmentation of semicircular canal geometry; bilateral pair)

Full 42-landmark protocol and bilateral mirror assignments available on MorphoSource Project M-659284.

Novel CT Character Descriptions (selected)

Character 1 (Skull roof trabeculation; family-level): Trabecular bone architecture in skull roof cross-section: (0) solid compact bone (Ichthyophiidae); (1) sparse trabecular lattice (Dermophiidae); (2) dense cancellous bone (Salamandridae)

Character 4 (Inner ear canal ratio; subfamily-level): Ratio of anterior semicircular canal diameter to posterior semicircular canal diameter: (0) < 0.8 (Hemidactyliini); (1) 0.8–1.0 (Plethodontini); (2) > 1.0 (Bolitoglossini)

Character 9 (Vertebral zygapophyseal angle; family-level): Angle between anterior zygapophyses and vertebral midline: (0) < 30° (Sirenidae); (1) 30–60° (Proteidae); (2) > 60° (all others)